PNAS
www.pnas.org

Supplementary Information for

# Guanine, a high-capacity and rapid-turnover nitrogen reserve in microalgal cells

Peter Mojzeš[1,2], Lu Gao[2,3], Tatiana Ismagulova[4], Jana Pilátová[5], Šárka Moudříková[1], Olga Gorelova[4], Alexei Solovchenko[4,6], Ladislav Nedbal[2*], Anya Salih[7]

Corresponding author: Ladislav Nedbal
Email: l.nedbal@fz-juelich.de

**This PDF file includes:**

Supplementary text
Figures S1 to S16
Table S1
Legend for Movie S1
SI APPENDIX References

**Other supplementary materials for this manuscript include the following:**

Movie S1

## I. Supplementary Information Text

**I.1. Localization of guanine, lipids, chloroplasts, and starch by Raman microscopy (Fig. 1 in the main text).** The images in Fig. S1 are complementary to those in Fig. 1 in the main text and show Raman maps of individual cell components in separate panels (D-O). The separate maps in Fig. S1 provide a more detailed information than the overlays in Fig. 1C–E (here repeated in Fig. S1 A-C). The method to obtain these maps is described in detail in SI APPENDIX II.1.C

**I.2. Kinetics of guanine accumulation and maximum storage capacity (Figs. 2 in the main text).** The mean amount of guanine accumulated per cell can be calculated from the drop in the guanine concentration in the supernatant (Fig. 2) and by normalization to cell density. We assumed that during the short uptake periods of our experimental treatments, the guanine was neither used for growth nor transformed into other chemical forms. This assumption was supported by the guanine accumulation analysis shown in Fig. 1.
Fig. S2 shows data used to calculate the guanine storage capacity of *A. carterae.* The most diluted experimental algal suspension (triangles in Figs. 2 and S2) took up only a fraction of the available guanine and by dividing this amount by the number of cells present, the resultant estimated maximal storage capacity of *A. carterae* cells was 143 ± 37 pg (guanine)·cell$^{-1}$.

**I.3. Raman spectra of various purines and stable-isotope-labelled guanines (Figs. 4 and 5 in the main text).** *Identification.* The chemical nature of the crystalline inclusions within cells was determined by comparing their Raman spectra with Raman spectra of reference samples (SI Appendix II.1.C.). Raman spectra of several purines, including crystalline guanine and uric acid, are shown in Fig. S4. Fig. S5 presents a comparison with various forms of uric acid. Raman spectra of calcite, calcium oxalate monohydrate, and calcium oxalate dihydrate that were earlier suspected to be present in algal inclusions are shown in Fig. S6.
*Deuterium-labelling*. Deuterated crystalline $d_1$-guanine, $d_4$-guanine, and $d_5$-guanine were used as reference samples. The materials and preparation are described in SI Appendix II.2.A. Raman spectra of these isotopically-labeled deuterium-guanine forms can be easily distinguished due to their distinct spectral fingerprints (Fig. S7).
*$^{15}$N-labelling.* To distinguish the N-source of guanine biosynthesized *de novo* from the compounds constituting N-sources in the media commonly used for microalgal cultivation (*i.e.*, nitrate, ammonium, urea), and to eliminate any doubt about the origin of the endogenous guanine, isotopically labeled $^{15}$N-compounds were used as the alternative N-sources. Consequently, $^{15}$N-guanine newly biosynthesized from specific exogenous $^{15}$N-sources was easily distinguished from the preexisting $^{14}$N-guanine or from $^{14}$N-guanine recycled from degraded cellular components. Spectral differences between Raman spectra of crystalline $^{14}$N- and $^{15}$N-guanine are highlighted in Fig. S8.

**I.4. In situ chemical identification of inclusions in diverse algal species (Tab.1 in the main text).** Diverse algal species listed in the table below together with their origin were tested in cultivation media and under conditions recommended for their cultivation by the source collections (Table S1) as further specified in SI Appendix II.3.

| Species | Origin. | Code |
|---|---|---|
| *Symbiodiniaceae* | Isolates. *Symbiodiniaceae* cells were isolated from tissues of various cnidarian species (*Aiptasia* sp., *Euphyllia paraancora*, *Rhodactis indosinensis*, *Sinularia asterolobata*, *Zoanthus* sp.) purchased from the local marine aquarium shops. Regardless of their origin, all *Symbiodiniaceae* cells contained crystalline guanine unless their host was exposed to long-term (at least 3 months) nitrogen deficiency. | |
| *Amphidinium carterae* | **MCNA** - National Center for Marine Algae and Microbiota, Bigelow, USA | CCMP1314 |
| *Chromera velia* | **MCNA** - National Center for Marine Algae and Microbiota, Bigelow, USA | CCMP2878 |

| | | |
|---|---|---|
| *Microchloropsis gaditana* | **NIES** - National Institute for Environmental Studies, Tsukuba, Japan | NIES-2587 |
| *Vacuoliviride crystalliferum* | **NIES** - National Institute for Environmental Studies, Tsukuba, Japan | NIES-2860 |
| *Vischeria* sp. | **CAUP** - Culture Collection of Algae of Charles University, Prague, Czech Republic | Q202 |
| *Trachydiscus minutus* | **CCALA** - Culture Collection of Autotrophic Organisms of the Institute of Botany of the Czech Academy of Science, Třeboň, Czech Republic | 838 |
| *Synura petersenii* | **CAUP** - Culture Collection of Algae of Charles University, Prague, Czech Republic | Q13 |
| *Lobosphaera incisa* | **CAUP** - Culture Collection of Algae of Charles University, Prague, Czech Republic | H4301 |
| *Desmodesmus quadricauda* | **CCALA** - Culture Collection of Autotrophic Organisms of the Institute of Botany of the Czech Academy of Science, Třeboň, Czech Republic | 463 |
| *Chlamydomonas reinhardtii* | **CRC** - Chlamydomonas Resource Center, University of Minnesota, St. Paul, USA | CC-1690 |
| *Dunaliella acidophila* | **CAUP** - Culture Collection of Algae of Charles University, Prague, Czech Republic | G301 |
| *Haematococcus pluvialis* | **CAUP** - Culture Collection of Algae of Charles University, Prague, Czech Republic | G1002 |
| *Klebsormidium flaccidum* | **NIES** - National Institute for Environmental Studies, Tsukuba, Japan | NIES-2285 |

**I.5 Detection of guanine in symbiotic dinoflagellates in intact corals and in extracted algae (Fig. 7 in the main text).** Following the enrichment of the artificial seawater (prepared from Reef Crystals sea salt, Aquarium Systems, Sarrebourg, France) in aquaria by 0.3 mM $^{15}N$-$NaNO_3$ as a sole source of N, the newly synthesized $^{15}N$-guanine crystals re-appeared within 24 hours inside endosymbionts of *Euphylia paraancora* as was documented by the respective Raman spectra (SI Appendix II.1.C.) that precisely distinguished between $^{14}N$- and $^{15}N$-guanine (Fig. 6C, Fig. S14C). To the best of our knowledge, this is the first *in situ* identification of crystalline guanine within the intact symbiotic zooxanthellae directly in tissues of several anthozoan species.
*Symbiodiniaceae* within *cnidarians* obtained from a commercial marine store and maintained under optimal nutrient conditions contained a considerable amount of guanine crystals (Fig. 7A, Fig. S14). When whole organisms (*e.g,*, *Euphyllia paraancora*) were subjected for four months to N-starvation under N-depleted conditions (combined nitrate, nitrite and ammonium concentration < 1 µM) with only autotrophic feeding, their symbiotic algae lost all guanine reserves, while the coral polyps showed a pronounced reduction in size and became pale (*i.e.*, bleached). N limitation is known to cause an increased accumulation of lipid bodies and floridean starch granules (1, 2), as well as the reduction of chloroplast volume in symbiotic dinoflagellates (Fig. 6B, Fig. S14B).
We also explored the presence of guanine in symbiotic dinoflagellates of *Acropora millepora*, a common coral species from the Great Barrier Reef (Australia), in colonies freshly collected from the reef (Heron Island, GBR) and in their explants, prepared from colony fragments, maintained in small closed system seawater aquaria. Symbionts were analyzed either *in situ,* in the host tissue, or as extracted cells cultivated in natural seawater (Fig. 7 D-F). The crystalline guanine inclusions were identified in both types of samples characterized by confocal Raman microscopy and correlated with the highly reflective properties of guanine visualized by confocal reflection microscopy (Figs. S15, and S16). Similar to observations of the free-living *A. carterae* and to symbiotic dinoflagellates from the store aquaria kept corals, the crystals of guanine were observed in very large quantities inside the guanine-fed *Symbiodiniaceae* of *A. millepora*, were almost absent in the N-starved samples and were present in low to moderate amounts in the extracted symbionts of corals freshly collected from the reef (Fig. S15).

**I.6 Confocal fluorescence and reflection imaging.** Confocal fluorescence microscopy is far more widely available in biological laboratories than Raman microscopy. Confocal imaging is fast,

with high-throughput, and confocal reflection images can be acquired along with the confocal fluorescent ones. Since Raman microscopy enables the precise *in situ* identification of the chemical nature of crystalline inclusions, we first tested the validity of (SI Appendix II.1.C) of the confocal reflection microscopy to image and quantify crystalline inclusions by corresponding measurement of the same samples by Raman imaging. By being more reflective/light scattering than other cell components, we showed that crystalline inclusions such as guanine can be easily visualized in reflection mode using a confocal fluorescence microscope. Thus, the inclusions in *Symbiodiniaceae* cells were first identified by Raman microscopy as guanine crystals and immediately after, cells from the same algal extracts were imaged by the confocal fluorescence microscope Leica TCS SP8 (Leica Microsystems, Germany) in reflection mode. Guanine accumulations were seen as crystal-like, highly light-scattering inclusions. All other organelles, e.g., the nucleus, the pyrenoid, the lipid droplets, the chloroplasts, and the accumulation bodies did not produce a reflection signal (Figs. S15 and S16).
Importantly, the reflection imaging technique enabled the visualization of crystalline deposits much faster than by Raman microscopy, however, this technique could not differentiate between crystalline guanine and other light scattering crystalline inclusions, *e.g.*, calcite, calcium oxalate or uric acid. A combination of both techniques would therefore be desirable for rapid, high-throughput studies.

## II. Supplementary Information: Materials and Methods

All chemicals were used for the preparation of media, the stable-isotope labeled $^{15}$N-$NaNO_3$, $^{15}$N-$KNO_3$, urea-$^{15}N_2$, $ND_4OD$, and DCl, as well as the crystalline nucleobases (adenine, guanine, xanthine, hypoxanthine and uric acid) were purchased from Sigma-Aldrich (St. Louis, MO, USA), unless other supplier was specified.

### II.1. Uptake kinetics of dissolved guanine and intracellular guanine inclusions of A. carterae (Figs. 1- 3 in the main text).

*II.1.A. Cultivation of A. carterae*

The marine dinoflagellate *Amphidinium carterae* was obtained from the National Center for Marine Algae and Microbiota (NCMAS, CCMP1314), Bigelow, USA. First, 1 L culture was grown in the closed photobioreactor FMT150 (PSI, Drasov, Czech Republic) in a full f/2 medium (composition shown below in II.1.Aa). The suspension was sparged by 0.2 $L \cdot min^{-1}$ filtered ambient air passed through a humidifier. The cultivation regime was 12 h light / 12 h dark illumination. The irradiance was 40 µmol (photons)$\cdot m^{-2} \cdot s^{-1}$ generated by blue- and red-light emitting diodes. The temperature of the suspension was kept constant at 20 °C. Minor losses of medium volume due to evaporation were replenished with distilled water. The culture growth was monitored spectrophotometrically and checked by cell counting.
*N-starvation.* A stationary culture grown with nitrate was harvested by centrifugation (2000 ×g, 3 min), washed by and suspended in N-deficient f/2 medium (composition in II.1.Aa.) and filtered through sintered glass filter (P100, Schott-Duran, Germany) to remove clumps of cells.
The culture remained largely synchronous and was N-starved for approximately one week. The suspension was split into equal 20 mL batches, transferred to 100 mL flasks (Schott-Duran), and placed on an orbital shaker in the growth chamber 350H (Sanyo, Osaka, Japan) at T= 20°C, illumination 40 µmol (photons) $m^{-2}$ $s^{-1}$. The cells were maintained in this N-free environment for additional five days to degrade all remaining guanine crystals. The absence of crystalline guanine was checked by Raman microscopy (SI Appendix II.1.C.) and by polarization microscopy (II.1.D.).

*II.1.Aa. ASW f/2 medium with and without N-source*

The f/2 medium was prepared from artificial seawater (ASW) according to (3) and its N-deficient variant contained: 400 mM NaCl, 10 mM KCl, 9 mM $CaCl_2 \cdot 2H_2O$, 20 mM $MgCl_2 \cdot 6H_2O$, 20 mM $MgSO_4 \cdot 7H_2O$ and 1.85 mM KBr, $3.62 \times 10^{-5}$ M $NaH_2PO_4 \cdot H_2O$, $1.06 \times 10^{-4}$ M $Na_2SiO_3 \cdot 9H_2O$, $1.17 \times 10^{-5}$ M $FeCl_3 \cdot 6H_2O$, $1.17 \times 10^{-5}$ M $Na_2EDTA \cdot 2H_2O$, $3.93 \times 10^{-8}$ M $CuSO_4 \cdot 5H_2O$, $2.60 \times 10^{-8}$ M $Na_2MoO_4 \cdot 2H_2O$, $7.65 \times 10^{-8}$ M $ZnSO_4 \cdot 7H_2O$, $4.20 \times 10^{-8}$ M $CoCl_2 \cdot 6H_2O$ and $9.10 \times 10^{-7}$ M $MnCl_2 \cdot 4H_2O$. The final concentrations of vitamins added into the autoclaved ASW f/2 from the stock solution were $2.96 \times 10^{-7}$ M thiamine HCl (vitamin B1), $2.05 \times 10^{-9}$ M biotin (vitamin H) and $3.69 \times 10^{-10}$ M cyanocobalamin (vitamin B12).

The full ASW f/2 medium used for cultures grown on nitrate as a sole source of N was prepared from the N-deficient f/2 by adding 0.882 mM $NaNO_3$. The media were stored in amber glass bottles at 20 °C and used for no more than 30 days after preparation.

*II.1.Ab. Medium with saturated guanine as a sole N-source*
The saturated solution (~35 □M, (4)) of neutral guanine without visible solid particles was obtained by dissolving a slightly excessive amount of solid guanine in N-deficient f/2 at 60°C (stirred for 30 min) that was cooled to 20°C and filtered through a 0.22 µm Millipore membrane filter (Merck, Kenilworth, NJ, USA). The f/2 medium saturated with dissolved guanine was stored in amber glass bottles at 20 °C and used for no more than 5 days after preparation.
*II.1.Ac. Feeding N-starved A. carterae by ground fish scales*
The f/2 medium enriched by fish scales was prepared by leaching 100 mg of ground dry fish scales (rainbow trout, Atlantic salmon) in 100 mL of the N-deficient f/2 medium (SI Appendix II.1.Aa.) at 25°C for 24 hours. The remaining large pieces of fish scales were removed in the form of precipitate.

*II.1.B. Determination of soluble guanine by UV-absorption spectrophotometer*
The dissolved guanine concentration in f/2 medium was determined spectrophotometrically using the absorption spectrophotometer Specord 250 (Analytik Jena, Jena, Germany) and its published extinction coefficient value (5). Standard spectroscopic quartz cuvettes (Hellma Analytics, Jena, Germany) with optical lengths of 10, 50 and 100 mm were used depending on the measured concentrations. Spectra between 210 – 400 nm were recorded to avoid artifacts that can occur with single wavelength measurements. For each measurement, aliquots of 5, 10, or 20 mL were centrifuged (14000 ×g, 1 min) and the supernatant was filtered through the 0.22 µm Millipore membrane filter (Merck, Kenilworth, NJ, USA) to remove suspended nanoparticles. We used N-deficient f/2 medium as a blank reference.

*II.1.C. Confocal Raman and confocal fluorescence - reflection microscopies*
*Sample preparation*. The specimens for all Raman measurements were prepared and treated according to the methodology described in detail elsewhere (6-8). The algal cells were harvested by centrifugation (2000 ×g, 10 – 30 s) of 1 – 2 mL of cell culture and excess medium was discarded. Each cell pellet and a small amount of remaining medium were mixed with an approximately equal volume of 2% w/v solution of low-gelling agarose (T = 30 – 40°C) in the respective medium. The agarose solution was used to prevent movement of cells during measurements and was prepared using the low melting/gelling agarose (melting T=65°C, gelling T=28°C) purchased from Carl Roth (Karlsruhe, Germany). Several microliters of the suspension were spread as a thin layer between a quartz slide and a quartz coverslip; wet edges were dried with blotting paper and sealed with a CoverGrip sealant (Biotium, Fremont, CA, USA).
To remove the autofluorescence of chlorophyll that obscured the Raman spectra, a wide-area low-power photobleaching of the entire cell by a defocused 532 nm laser beam was applied prior to the mapping, as described previously (6). The mean guanine content per cell was quantified by Raman microscopy by measuring 5 – 12 randomly selected cells for each time point.
For confocal analysis the symbiotic algae were extracted from *Zoanthus* sp and *A. millepora* by excising and abrading tissues with a brush into filtered seawater (FSW). They were first cleaned of debris by passing through a fine nylon mesh and were further cleaned by repeated centrifugation and resuspension of the pelleted algae in FSW. A drop of microalgal suspension (A. *carterae, Zoanthus sp, A. millepora)* was placed on a glass slide under a glass coverslip for confocal analysis and for each, several slides were analysed with a total of 28-34 cells analysed from each culture or organism, and per treatment for *A. millepora*.
*Raman microscopy.* The quantitative dynamic studies of guanine biosynthesis and uptake by N-starved *A. carterae* were carried out using an inverted Raman microscope LabRam Evolution (Horiba Scientific, Longjumeau, France) with 532 nm laser excitation (10 mW power at the focal plane) and using the water-immersion objective Plan Apo VC 60×, NA 1.20 (Nikon, Minato, Japan). The spectrograph was equipped with a 150 gr/mm grating providing spectral resolution of 9 $cm^{-1}$. Raman mapping was conducted with 500 nm steps in both directions, and with two accumulations, each of 0.3 s integration time at each voxel. The apparatus was controlled by a

LabSpec 6 software (Horiba Scientific, Longjumeau, France). Further details of the apparatus were described elsewhere (6). After the format conversion, spectra were treated and analyzed by a home-made GNU Octave software (9) as described previously (8).
All other Raman measurements were conducted using an upright Raman microscope WITec alpha 300 RSA (WITec, Ulm, Germany) with a 532 nm laser excitation (20 mW power at the focal plane), an oil-immersion objective UPlanFLN 100×, NA 1.30 (Olympus, Shinjuku, Japan) and the spectrograph providing spectral resolution of 6 $cm^{-1}$. Scanning step in *x*- and *y*-direction was 200 nm, with an integration time of 0.1 s per voxel. Further details on the apparatus can be found in (8).
The acquired Raman spectra were treated, and the Raman chemical maps constructed by multivariate decomposition of the baseline-corrected spectra into the spectra of pure chemical components by using WITec Project Plus 5.1 software (WITec, Ulm, Germany). No differences that could affect data interpretation were observed between the results obtained with Horiba and with WITec Raman microscopes.
*Confocal microscopy*. For each analysis, we used Leica TCS SP5 or Leica TCS SP8 (Leica Microsystems, Heidelberg, Germany) inverted microscopes. Fluorescence imaging was by 63x water immersion objective (Plan-Apo, 1.2 NA) at excitation by Argon laser 488nm line and capturing the emission bands at 500 – 560 nm for organelles as the accumulation body and at 670-700nm for chlorophyll in two photomultiplier tubes (PMTs). Reflection from guanine was simultaneously imaged by excitation at 488nm, with the third PMT detection range centered on the laser line at 485-489nm to capture scattered wavelengths from crystals. Images were taken at approximately mid-depth into each cell at 512x512 pixel resolution.

*II.1.D. Polarization microscopy*
To acquire images and videos in polarized light, a polarizing accessory of the upright Raman microscope WITec alpha 300 RSA (WITec, Ulm, Germany) was used. The videos visualizing the fast formation of crystalline guanine within *A. carterae* cells were taken by WITec Project Plus 5.1 software (WITec, Ulm, Germany).
The N-starved *A. carterae* cells were immobilized between a glass slide and a glass coverslip by low-melting agarose (SI Appendix II.1.C) of approximately 100 □m thickness, without sealing the coverslip edges. Several drops of guanine-enriched f/2 medium (II.1.Ab.) were placed at the coverslip edges and the microalgae located near the edges were monitored through the crossed polarizes. As the dissolved guanine diffused towards the nearby algae, its uptake was confirmed by a considerable amount of crystalline guanine appearing inside them. The rapid accumulation was visualized by the strong light depolarization by newly formed crystals as early as within 14 minutes after the guanine solution was added (Movie S1).

*II.1.E. Ultrastructural transmission electron microscopy (TEM)*
The microalgae for TEM were fixed in 2% v/v glutaraldehyde solution in culture medium at room temperature for 0.5 h and then post-fixed for 4 h in 1% (w/v) $OsO_4$ in the 0.1 M sodium cacodylate buffer. The samples, after dehydration through graded ethanol series including anhydrous ethanol saturated with uranyl acetate, were embedded in araldite. Ultrathin sections were made with an LKB-8800 (LKB, Sweden) ultratome, mounted to the formvar-coated TEM grids, stained with lead citrate according to Reynolds (10) and examined under JEM-1011 (JEOL, Tokyo, Japan) microscope.

*II.1.F. Energy-dispersive X-ray spectroscopy (EDX)*
The samples for nanoscale elemental analysis in analytical TEM using EDX were fixed, dehydrated and embedded in araldite as described above, excepting the staining with uranyl acetate and lead citrate. Semi-thin sections were examined under JEM-2100 (JEOL, Japan) microscope equipped with a $LaB_6$ gun at the accelerating voltage 200 kV. Point EDX spectra were recorded using JEOL bright-field scanning TEM (STEM) module and X-Max X-ray detector system (Oxford Instruments, UK). The energy range of recorded spectra was 0–10 keV with a resolution of 10 eV per channel. At least ten cells per specimen were analyzed. Spectra were processed with INKA software (Oxford Instruments, UK) and presented in a range 0.1-4 keV.

**II.2. Combining isotopic-labelling with Raman microscopy (Fig.4 and 5 in the main text).**

*II.2.A. Deuterated guanine for uptake solid guanine experiments (Fig. 4 in the main text).*

Heavy water ($D_2O$, 99.9%) used in the experiments was purchased from Silantes (München, Germany). Deuterated $d_1$-guanine (8)D, $d_4$-guanine (1,2,2,9)D and $d_5$-guanine (1,2,2,8,9)D were prepared from crystalline guanine (Sigma-Aldrich) according to the procedure described in (11). The isotopic purity of $d_1$-, $d_4$-, and $d_5$-guanine was checked by Raman microscopy (SI Appendix II.1.C.) and compared with the corresponding spectra reported in (11).

The base media and studied organisms were the same as described above in relation to Figs. 1-3. The methodological approach is described in the main text, and in further detail in SI Appendix. II.1.A for cultivation and SI Appendix II.1.C. for Raman measurements.

*II.2.B. $^{15}$N-sources for cell growths and guanine dynamics (Fig. 5 in the main text).*

For *de novo* biosynthesis experiments, various $^{15}$N-labeled compounds constituting N-sources in the media commonly used for microalgae cultivation were tested. The stable-isotope labeled $^{15}$N-$NaNO_3$, $^{15}$N-$KNO_3$ and urea-$^{15}N_2$ were purchased from Sigma-Aldrich (St. Louis, MO, USA). The $^{15}$N-$NH_4Cl$ was acquired from Silantes (München, Germany). The stable-isotope fully-labeled crystalline $^{15}$N-guanine was prepared from commercially available guanosine-$^{15}N_5$ 5′-monophosphate, sodium salt, (Sigma-Aldrich) by acid hydrolysis of the N-glycosidic bond (12) and subsequent neutralization by NaOH. The precipitated neutral $^{15}N_5$-guanine ($^{15}$N-guanine) was washed by deionized water and dried. The isotopic purity was checked by Raman microscopy (SI Appendix II.1.C.) and compared with the corresponding spectrum reported in (11). The spectral differences between $^{15}$N- and $^{14}$N-guanine are shown in Fig. S8. The frequency downshifts by 5 – 20 $cm^{-1}$ caused by the heavier $^{15}$N atoms largely exceeded the experimental error (< ±1 $cm^{-1}$) and enabled a straightforward and an unambiguous identification of the respective species.

The media and the organisms used for the biosynthesis and uptake experiments were as described above in relation to Figs. 1-3. The 20 mL batches (in triplicate) of the N-starved *A. carterae* cells (II.1.A.) were supplemented with various $^{15}$N-sources.

To provide the same amounts of N atoms regardless of the N-source, we added either $^{15}$N-nitrate to the final concentration of 0.882 mM corresponding to the full f/2 medium (54.69 $mg \cdot L^{-1}$), or 0.882 mM $^{15}$N-ammonium (15.91 $mg \cdot L^{-1}$), or 0.441mM $^{15}$N-urea (26.48 $mg \cdot L^{-1}$) or 0.1764 mM $^{15}$N-guanine as the sole N sources. Nitrate, ammonium and urea were added in the form of 1000-fold concentrated solution. Guanine was added as a solid powder (0.53 mg per 20 mL cell suspension) because of its limited solubility.

The cell density and average cell size were measured in triplicate by the Coulter counter Multisizer 3 (Beckman Coulter, Brea, CA, USA) with a 100 µm aperture or by using Bürker counting chamber (n=9).

The mean guanine content per cell was quantified by Raman microscopy measuring 5–12 randomly selected cells for each time point.

In other methodological aspects, our approach is further described in detail in the main text, in SI Appendix II.1.A for cultivation and SI Appendix II.1.C. for Raman measurements.

**II.3. Source and maintenance of free-living microalgae (Tab. 1 in the main text).**

The free-living marine algal species were cultivated in a full ASW f/2 medium prepared from N-deficient f/2 (SI Appendix II.1.Aa.) enriched by $8.82 \times 10^{-4}$ M $NaNO_3$ as a sole source of N (3). The freshwater microalgae were cultivated in the Bold's Basal Medium (BBM) (13), ½SŠ medium (14), BG-11 medium (15) or media recommended by the supplier of the algal strain. None of the media used for basic screening was enriched with guanine or other purines.

**II.4. Source and maintenance of symbiotic microalgae (Fig. 7 in the main text).**

*II.4.A. Symbiodiniaceae from aquaria-kept anthozoans (Fig. 7 A–C in the main text).*

Various cnidarian species, *e.g.*, anemone *Aiptasia* sp., corallimorpharian *Rhodactis indosinensis*, scleractinian coral *Euphyllia paraancora*, leather coral *Sinularia asterolobata*, and *Zoanthus* sp. were obtained from a marine aquarium store.

They were maintained in small experimental aquaria (8 L, closed circulation of filtered water, 25 °C, 12h/12h light/dark cycle, 100 µmol(photons)$\cdot m^{-2} \cdot s^{-1}$ illumination by white- and blue-light emitting diodes) under controlled nutrient conditions in the artificial marine water prepared from

the Reef Crystals sea salt (Aquarium Systems, Sarrebourg, France) according to the manufacturer's instructions and supplemented with trace elements by a weekly dosage of commercially available solutions Coral Colours (Red Sea, Eilat, Israel).
Commercially available colorimetric Profi Test kits (Salifert, the Netherlands) were used to test and maintain the pH, carbonate hardness/alkalinity, concentrations of nitrate, nitrite, ammonia, and phosphate according to the manufacturer's instructions. The resultant color changes were quantified by the absorption spectrophotometer Specord 250 (Analytik Jena, Germany) and *via* calibration based on the concentration series of the respective compounds.
The chemical nature of the crystalline inclusions of anthozoan endosymbionts were first analysed immediately after acquisition, and subsequently, at regular intervals, by excising a small piece of soft tissue, positioning it between glass microscope slide and coverslip, and immediately analyzing by Raman microscopy (SI Appendix II.1.C.).

*II.4.B. Symbiodiniaceae from reef collected coral Acropora millepora (Fig. 7* D–F *in the main text).*
Replicate explants from four *A. millepora* colonies were starved in N-depleted artificial seawater in experimental aquaria for 4 weeks. Dinoflagellate symbionts were extracted by repeated centrifugation and filtering, cultured in nutrient depleted media for additional 4 days, analyzed by confocal reflection microscopy and compared to cells one day later following the addition of crystalline guanine to the artificial seawater and to symbionts extracted from three *A. millepora* that were used for analysis immediately after reef collection and transportation to the laboratory.

**III. Supplementary Information: Results**

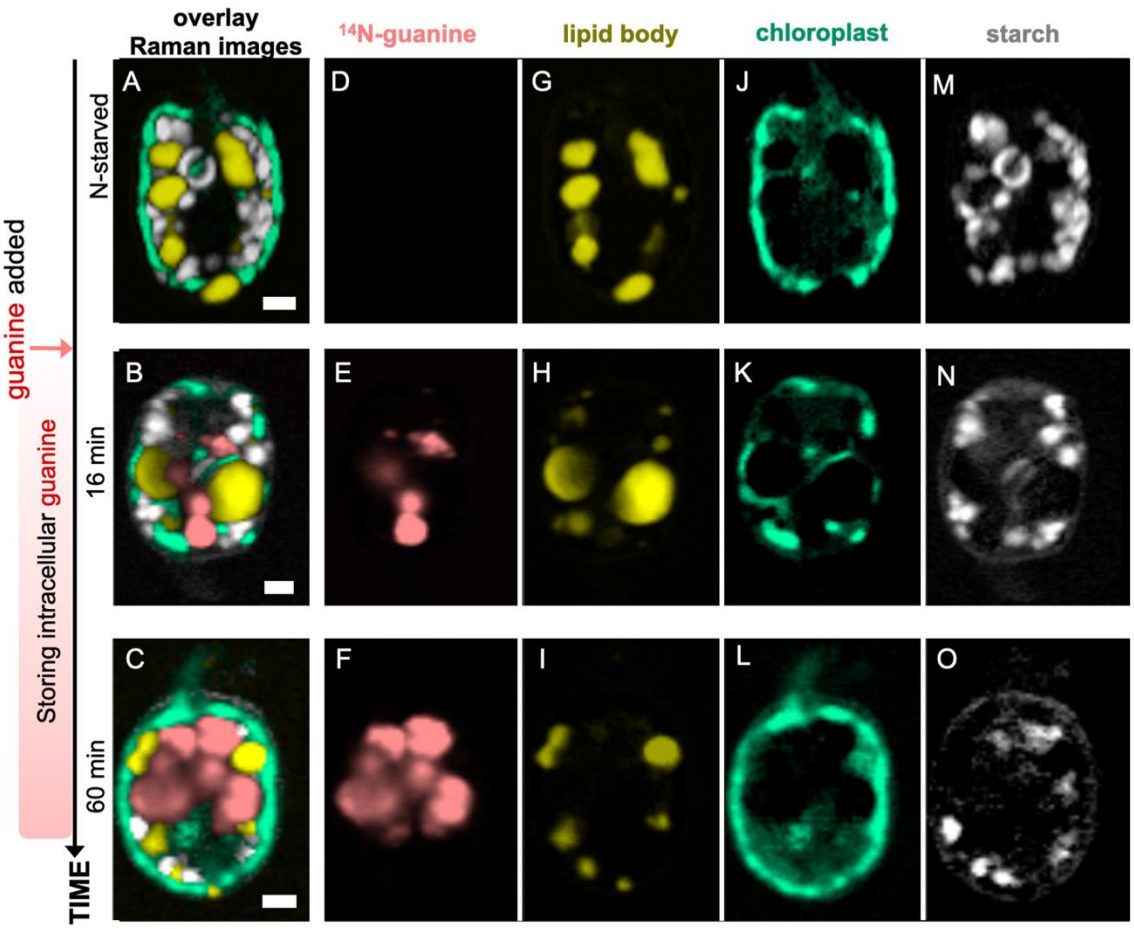


**Fig. S1 (complementing Figs. 1C–E). Rapid uptake of guanine by N-starved *A. carterae* led to accumulation of intracellular guanine inclusions.** The combined Raman maps (A–C) represent typical cells after two weeks of N-starvation (first row) and cells during progressive guanine accumulation (second and third rows). Intracellular distribution of crystalline guanine (D–F), neutral lipids (G–I), chloroplasts (J–L) and floridean starch (M–O) are shown in separate panels for clarity. The corresponding Raman spectra are shown in Fig. 1B. Scale bar: 2 µm.

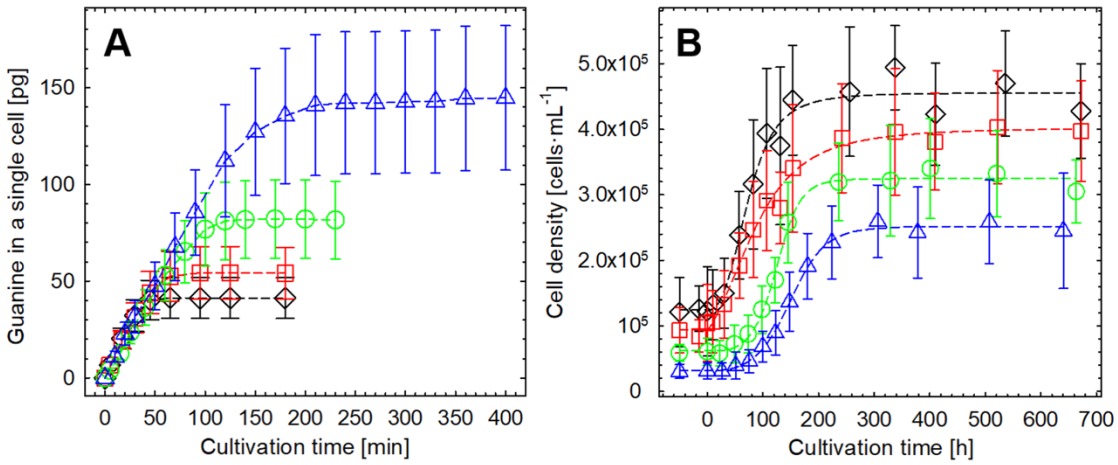


**Fig. S2 (complementing Fig. 2). Rapid uptake of guanine by N-starved *A. carterae* and subsequent growth of the culture at the expense of accumulated stocks. (A)** Accumulation of guanine reserves inside cells estimated from the uptake kinetics shown in Fig. 2. The cell densities were (12.2 ± 3.1*) × $10^4$ cells·$mL^{-1}$ (◇), (9.3 ± 2.3) × $10^4$ cells·$mL^{-1}$ (□), (6.1 ± 1.5) × $10^4$ cells·$mL^{-1}$ (◯), and (3.1 ± 0.8) × $10^4$ cells·$mL^{-1}$ (△). The cells of the most diluted culture (△) did not take all of the dissolved guanine from the medium, thus indicating that their maximum storage capacity was 143 ± 37 pg of crystalline guanine.
**(B)** Growth of cell cultures influenced by guanine reserves generated by the rapid uptake shown in **A**. Cultures were cultivated under identical conditions until they reached a new stationary phase. Their growth was monitored by cell counting (Bürker counting chamber; 2 replicates, 18 readouts). From the initial cell densities (12.2 ± 3.1) × $10^4$ cells·$mL^{-1}$ (◇), (9.3 ± 2.3) × $10^4$ cells·$mL^{-1}$ (□), (6.1 ± 1.5) × $10^4$ cells·$mL^{-1}$ (◯), and (3.1 ± 0.8) × $10^4$ cells·$mL^{-1}$ (△), the final cell densities increased by 3.7 ± 1.1, 4.2 ± 1.4, 5.3 ± 1.7 and 8.1 ± 3.1 times, respectively. The growths were fitted to five-parameter logistic function (RSQR ≥ 0.985).
*a number that follows the ± sign is a standard deviation (SD) in this work.

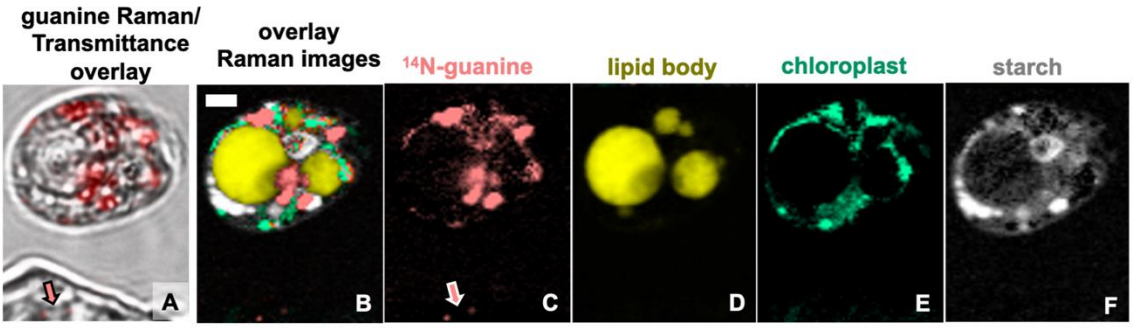


**Fig. S3. N-starved *A. carterae* fed by ground fish scales.** Bright field image (A) overlaid by guanine Raman map which is shown separately in panel C. Multicomponent Raman chemical map (B). Individual Raman maps of crystalline guanine (C), neutral lipids (D), chloroplasts (E) and floridean starch (F).
Outside the cell, a piece of fish scale containing a small amount of guanine is indicated by the pink arrows in (A) and (C). The cell was mapped 60 min after leachate from the fish scales was added. Raman mapping was conducted in dozens of replicates; a representative cell is shown. Scale bar: 2 μm.
The f/2 medium enriched with leachate from fish scales was prepared by maintaining 100 mg of ground dry fish scales (rainbow trout, Atlantic salmon) in 100 mL of the N-deficient f/2 medium at 25°C for 24 hours. The N-starved cells were transferred to the leachate cleaned free of coarse pieces of sediments. The presence of guanine was confirmed by Raman microscopy of 5 or more of randomly selected cells.

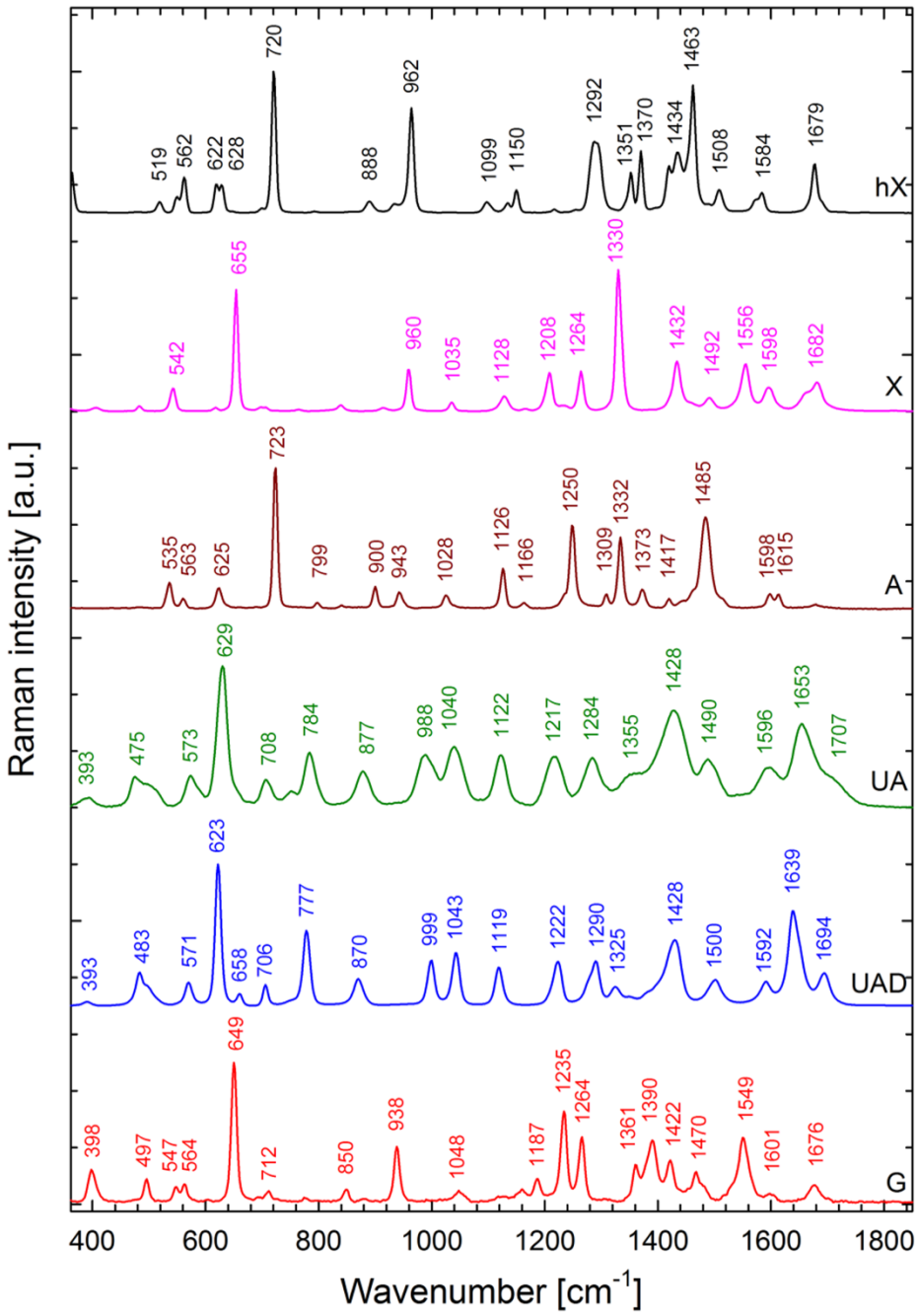


**Fig. S4.** Comparison of Raman spectra of crystalline anhydrous guanine (G) and crystalline forms structurally related purine bases (adenine – A; xanthine – X; hypoxanthine – hX; uric acid – UA, UAD). The spectrum UA shows uric acid detected in microalgae (*e.g.*, *Klebsormidium flaccidum*) and UAD shows the most similar spectrum of a single crystal of uric acid dihydrate for a specific crystal orientation. Uric acid present in some microalgae species could not be easily identified by means of the reference spectrum of polycrystalline anhydrous uric acid (see Fig. S5 for details). For the sake of clarity, only the range of characteristic vibrations (360 – 1850 $cm^{-1}$) is shown.

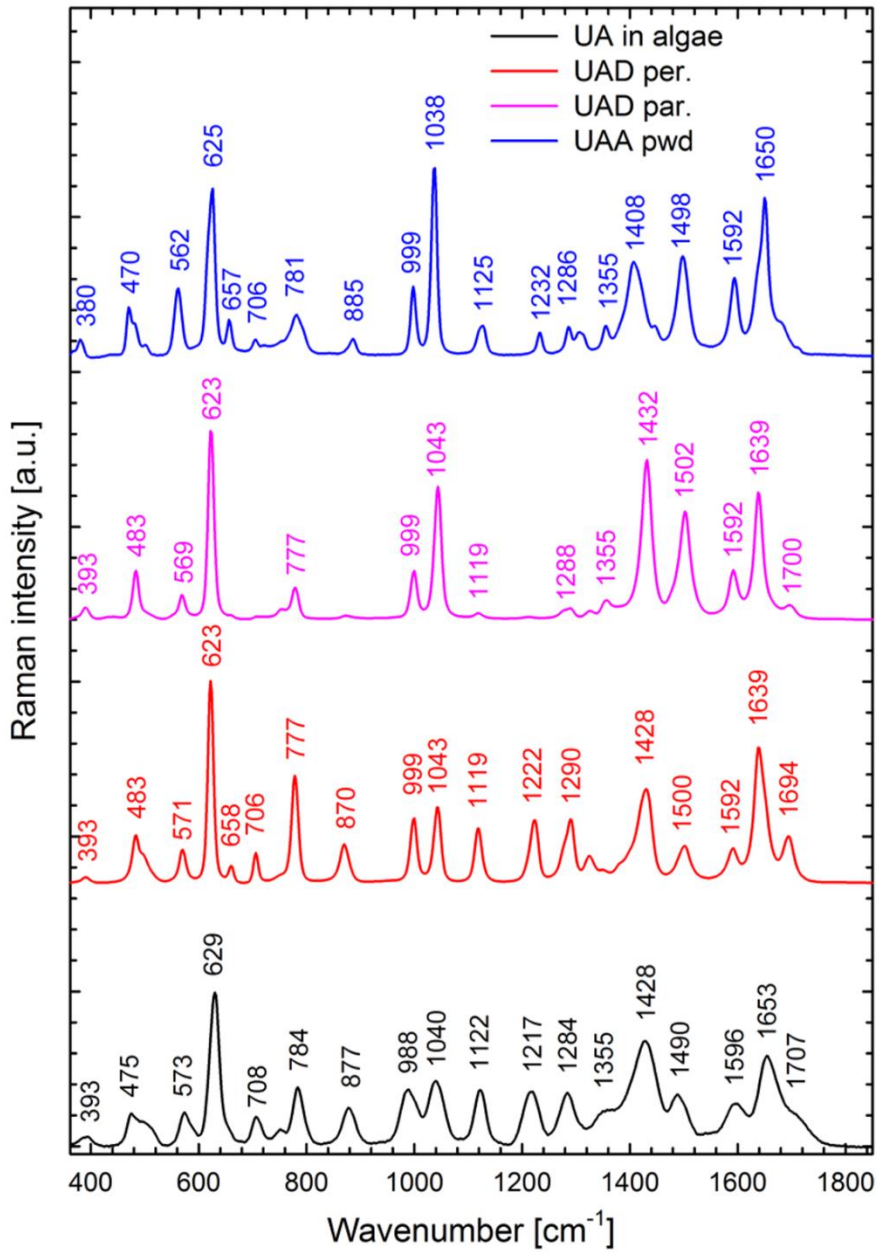


**Fig. S5.** Comparison of Raman spectra of different crystalline forms of uric acid. Uric acid was commercially available as an anhydrous polycrystalline powder (UAA pwd, blue line) from which it can be recrystallized under specific conditions to anhydrous or dihydrate single crystals (16). Unlike the polycrystalline UAA powder, the relative intensities of the Raman bands of single crystals were sensitive to the orientation of their flat plate faces with respect to the electric vector of the excitation beam, as was evidenced by the spectra of dihydrate uric acid single crystal oriented parallelly (UAD par, magenta line) and perpendicularly (UAD per, red line). Raman spectra of uric acid detected in microalgae (UA in algae, black line) were most similar to the spectrum of UAD per., nevertheless, Raman bands were broader, indicating a less strict crystal packing of the molecules.

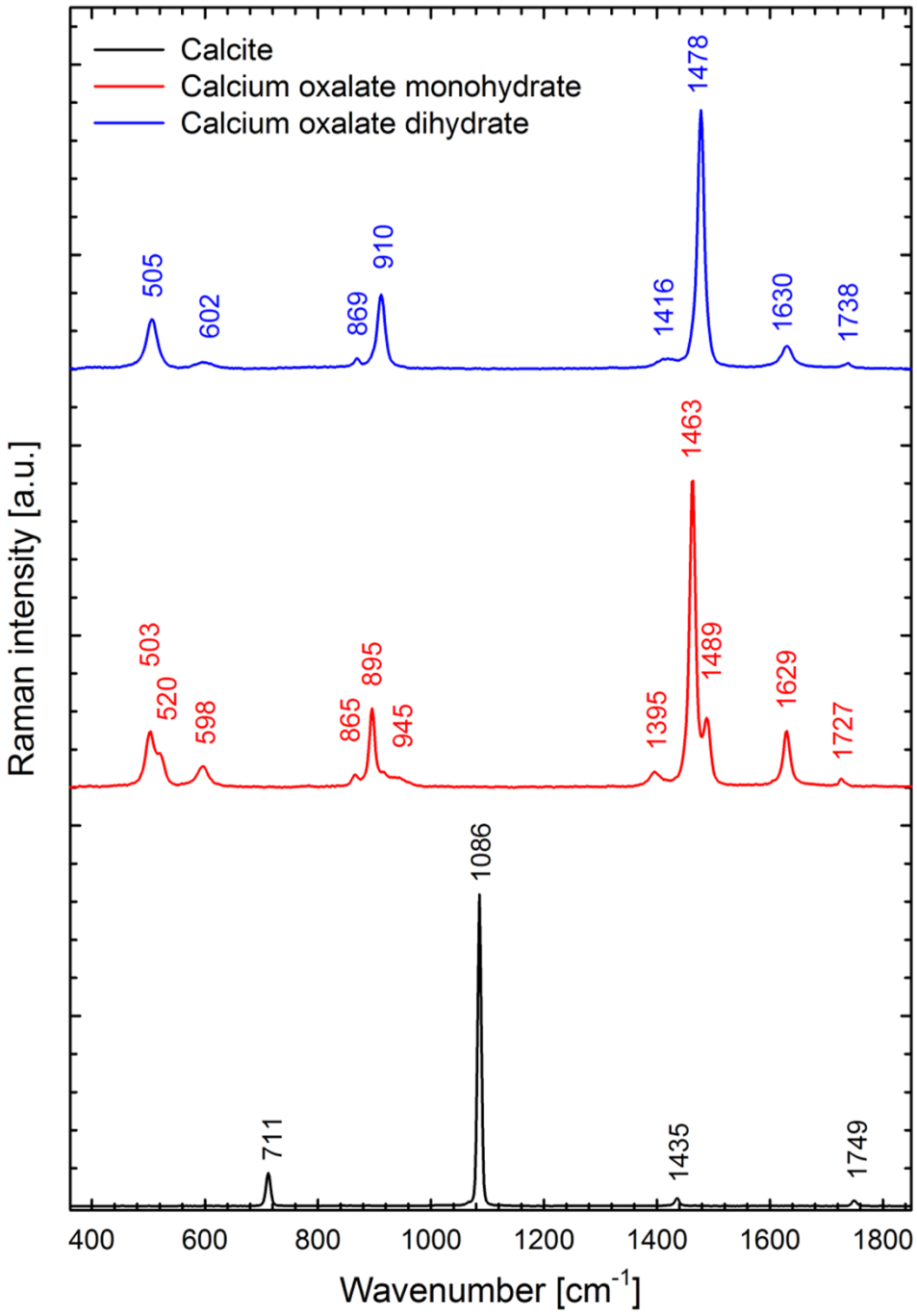


**Fig. S6.** Raman spectra of calcite, calcium oxalate monohydrate, and calcium oxalate dihydrate.

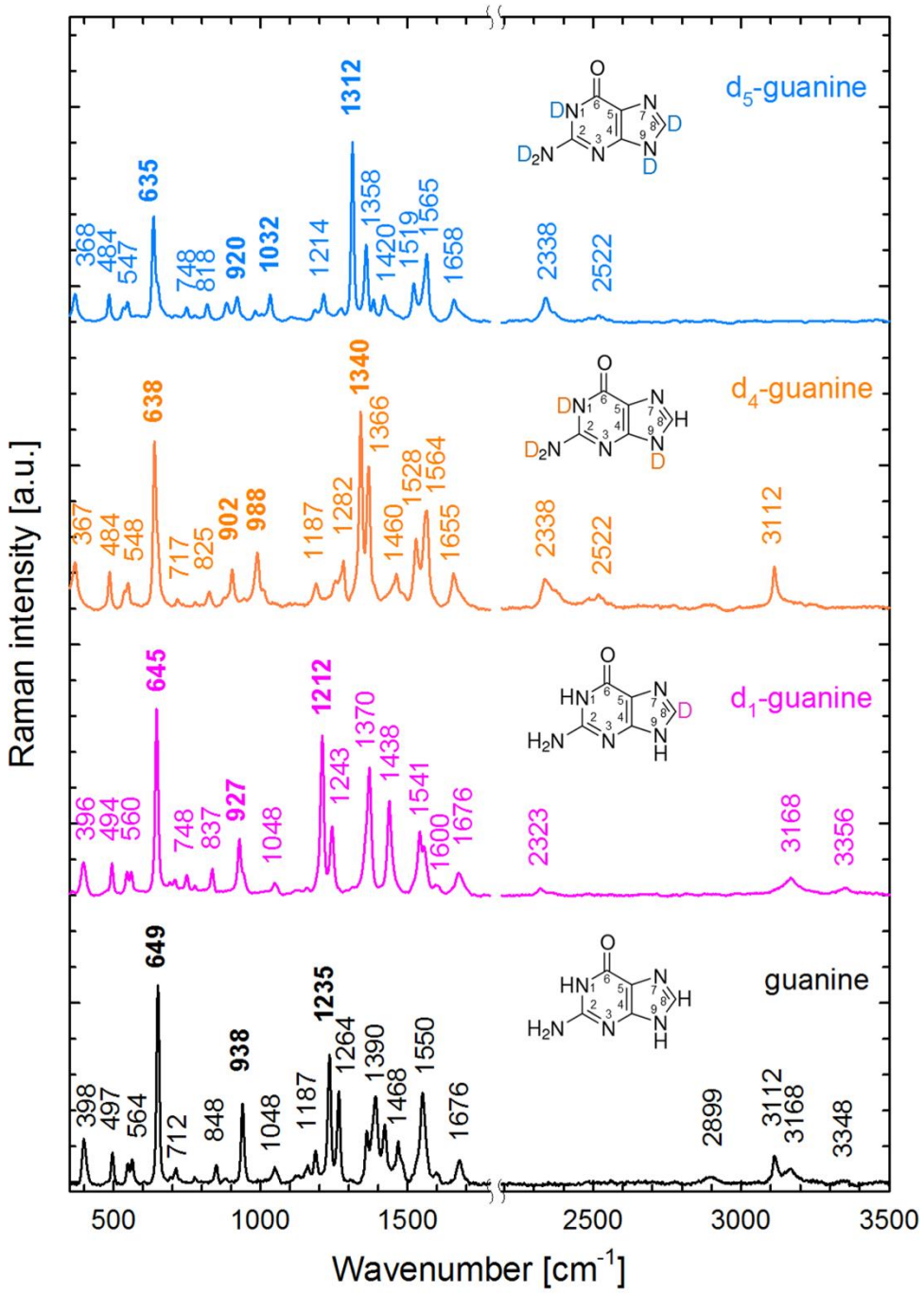


**Fig. S7 (complementing Fig. 4).** Raman spectra of normal guanine and its deuterium-labeled derivatives.

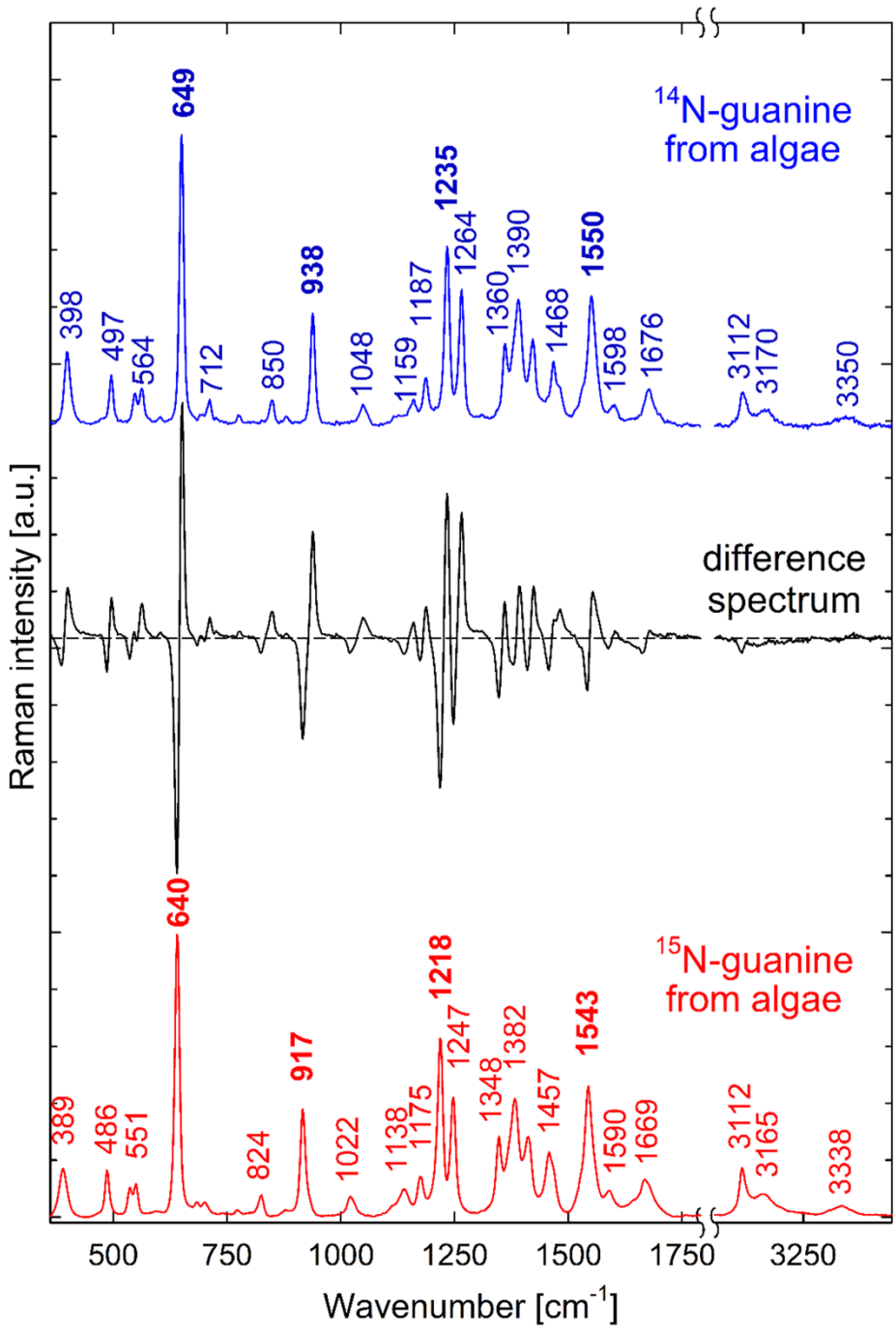


**Fig. S8 (complementing Fig. 7).** Direct comparison of Raman spectra of crystalline $^{14}$N- and $^{15N}$-guanine. To highlight the specific isotopic frequency shifts between both isotopic guanine species, the difference spectrum is shown for clarity. The differences in wavenumbers of individual bands of the $^{14}$N- and $^{15}$N-guanine were found sufficiently large for a reliable discrimination by Raman spectroscopy. In fact, the shifts were as large as 5–20 cm$^{-1}$, while the spectral resolution of our Raman spectrometer was better than ± 1 cm$^{-1}$.

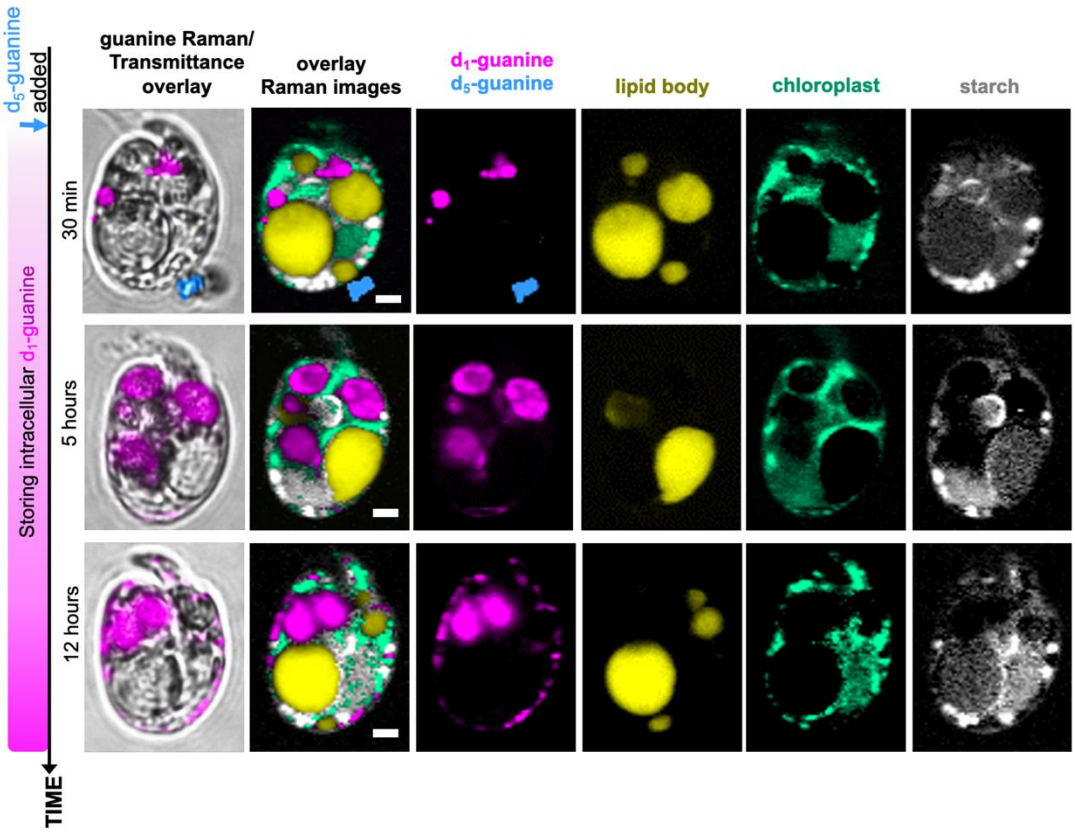


**Fig. S9 (complementing Fig. 4). Uptake of guanine includes the exchange of deuterium for hydrogen atoms.** Bright field images overlaid by guanine Raman maps (A, B, C), multicomponent Raman maps (D, E, F) and Raman maps of the most important components (G–R) of the N-starved *A. carterae* after the addition of solid crystalline $d_5$-guanine into N-depleted medium. Images collected 30 min, 5 hours and 12 hours after $d_5$-guanine addition. Raman maps of $d_5$- and $d_1$-guanine (G–I) are represented in blue and magenta, respectively, both in the corresponding Raman spectrum (Fig. S7) and in the images. Other colors: yellow – neutral lipids, green – chloroplasts, gray – floridean starch. Scale bars (D–F): 2 μm.

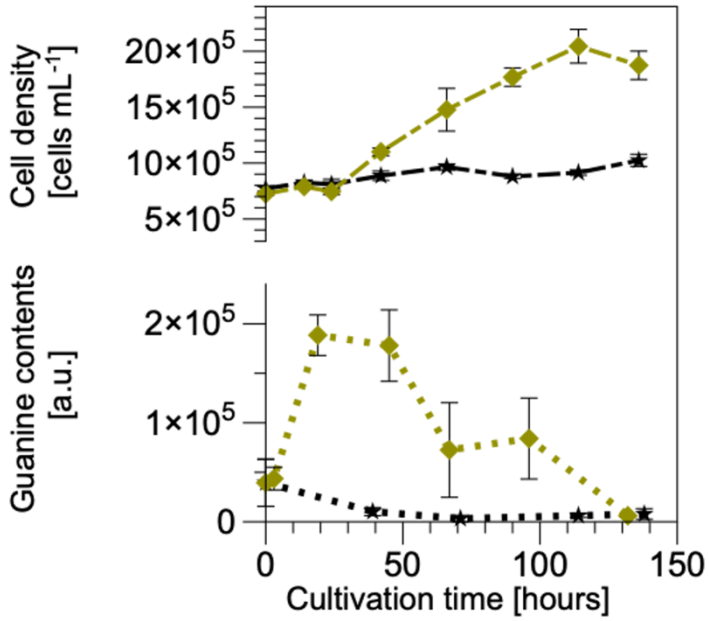


**Fig. S10 (complementing Fig. 5). Nitrogen in $^{15}$N-guanine inclusions originated directly from the supplied $^{15}$N-labelled urea.** *A. carterae* cell density stagnated in the control samples without N-feeding (black line, upper graph) and resumed growth after the addition of $^{15}$N-labelled urea at concentration of 0.882 mM (N) (yellow line, upper graph). The corresponding intracellular crystalline guanine contents per cell are shown in the bottom graph representing Raman measurements of 5–12 cells.

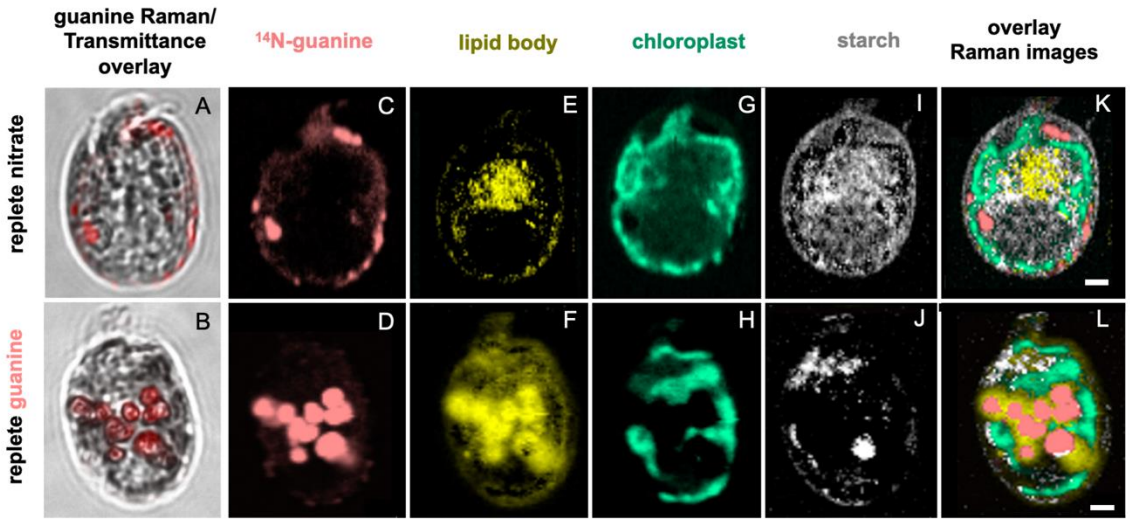


**Fig. S11 (complementing Fig. 6). Localization of guanine inclusions in *A. carterae* fed by nitrate (top row) or guanine (bottom row) after 24 hours.** Bright field images overlaid by guanine Raman maps (A, B). Separate Raman maps of guanine (C, D), neutral lipids (E, F), chloroplast (G, H), and floridean starch (I, J). Combined multicomponent Raman chemical map (K, L). Scale bar: 2 µm.

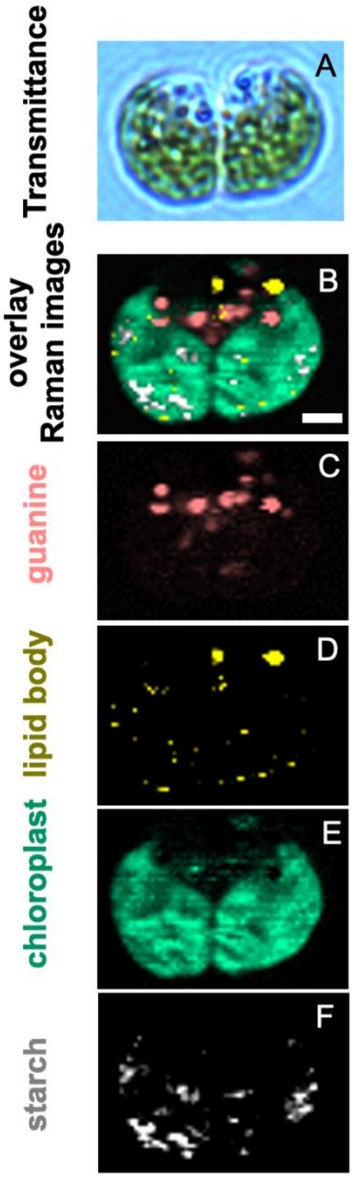


**Fig. S12. Crystalline guanine inclusions in the dividing *Chlamydomonas reinhardtii*.** Bright field image (A), multicomponent Raman chemical map (B), separate Raman map of guanine (C), neutral lipids (D), chloroplasts (E), and starch (F). Scale bar: 2 μm.

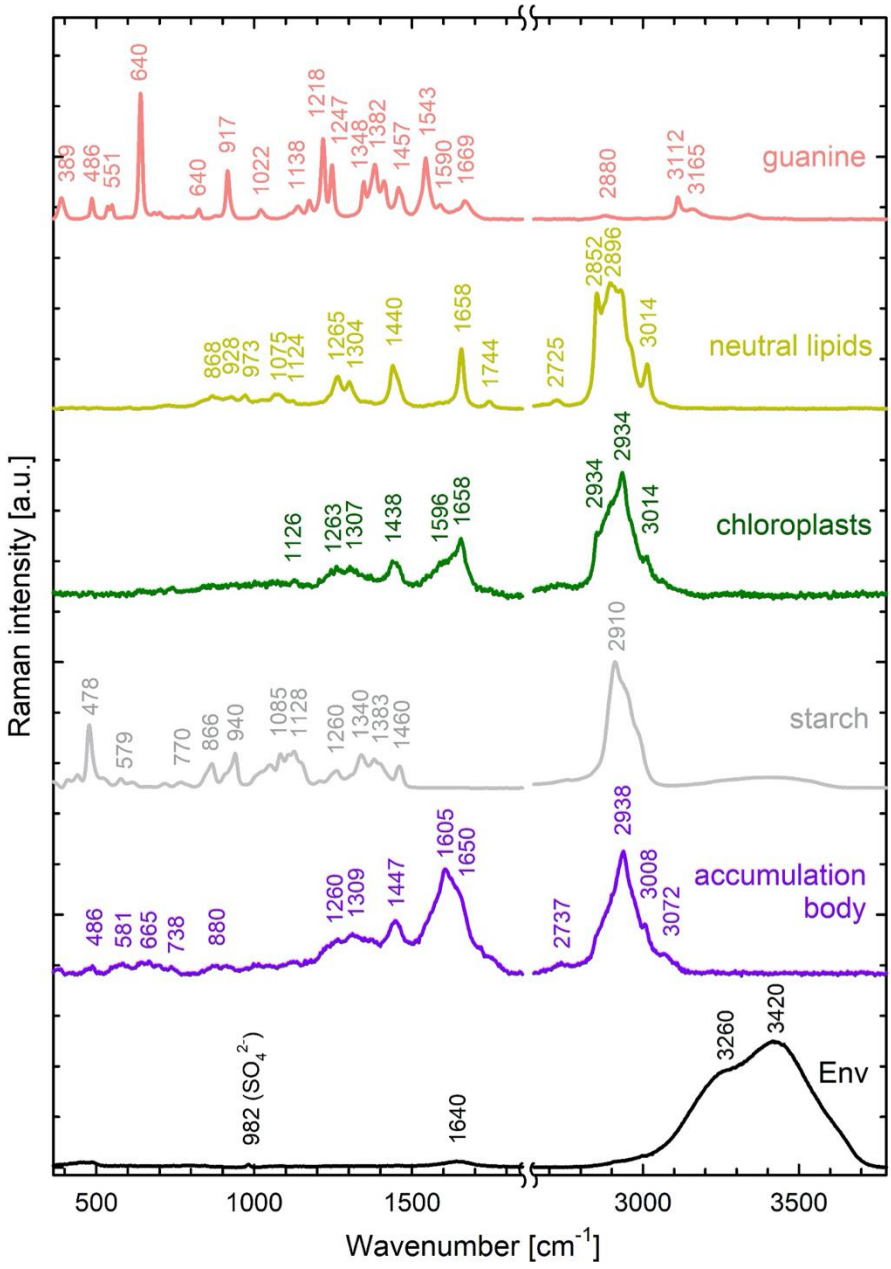


**Fig. S13 (complementing Fig. 7). Raman spectra of pure components identified in *Symbiodiniaceae* cells re-fed with $^{15}N$-$NaNO_3$.** The full–range Raman spectra of crystalline $^{15}N$-guanine, neutral lipids, chloroplasts, floridean starch, accumulation body, and seawater surrounding the cell were used for multivariate decomposition of Raman maps of *Symbiodiniaceae* cells and construction of chemical maps shown in Fig. 7.

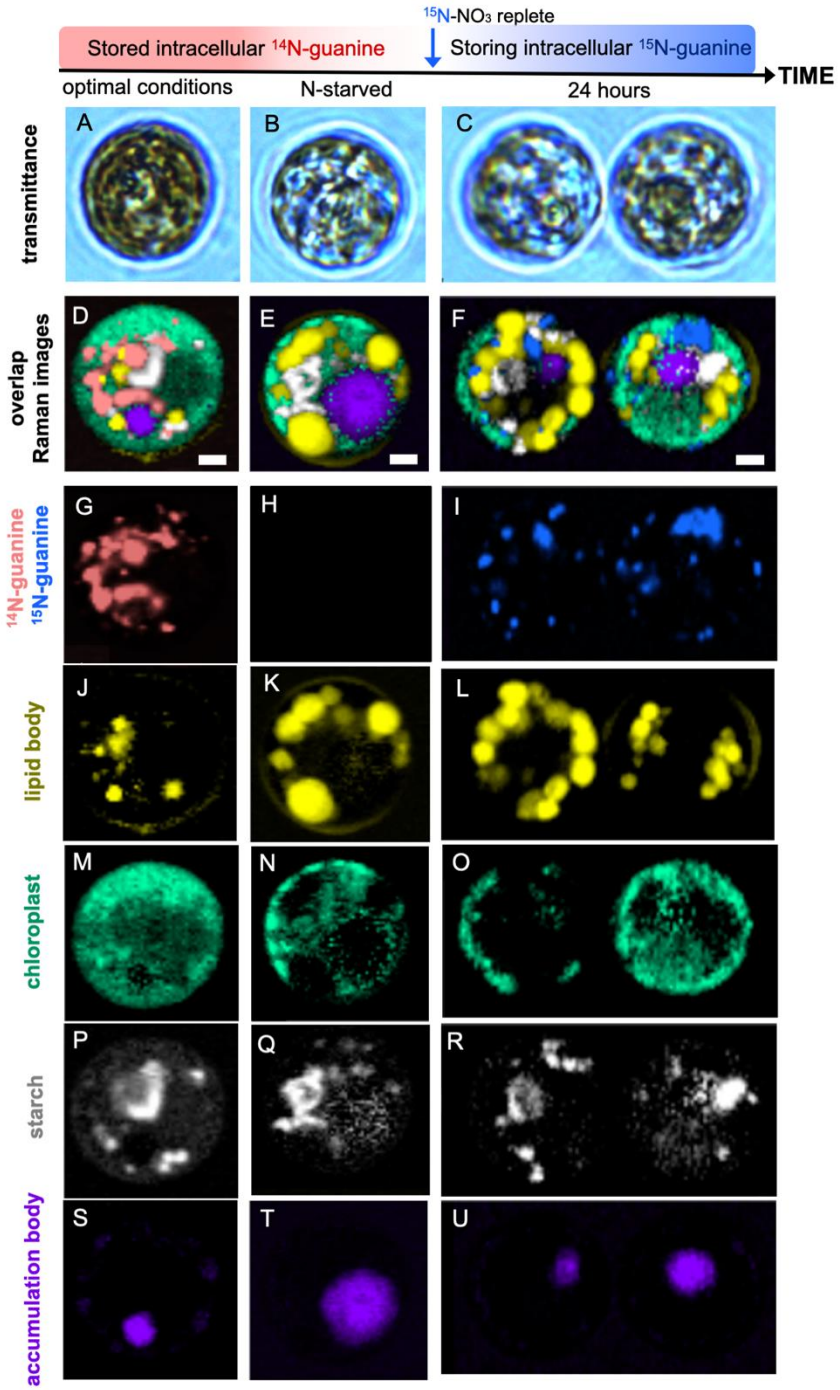


**Fig. S14 (complementing Fig. 7). Raman chemical maps of *Symbiodiniaceae* cells extracted from the tissue of the coral *Euphylia paraancora.*** *Algae* from corals cultivated under optimal nutrient conditions in an aquarium shop contained guanine crystals (D, G). After four-month cultivation of the entire holobiont in N-depleted seawater, they lost their guanine reserves (E, H). When corals were transferred into seawater enriched by 0.3 mM $^{15}$N-NaNO$_3$, newly synthesized $^{15}$N-guanine crystals appeared within 24 h (F, I) in algae as documented by the highly specific Raman spectra clearly distinguishing between $^{14}$N- and $^{15}$N-guanine (Fig. S8). Raman mapping was replicated (n=12 or more cells) and conducted on three holobiont replicates; representative cells are shown. Scale bar: 2 μm.

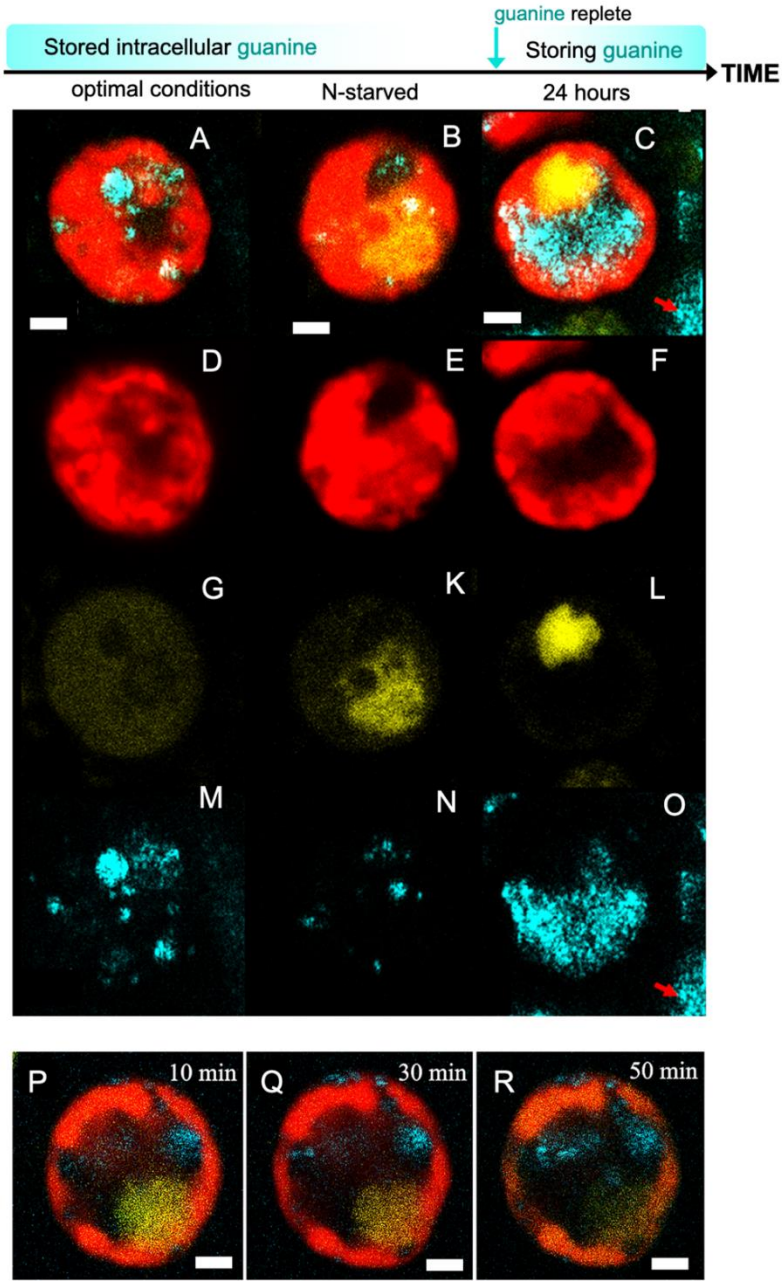


**Fig. S15 (complementing Fig. 7). Confocal fluorescence and reflectance images of *Symbiodiniaceae* cells extracted from the coral *A. millepora***. Combined images (A–C), chlorophyll fluorescence 670 – 700 nm (D–F), fluorescence at 500 – 560 nm assigned predominantly to accumulation body (G–L), and 488 nm reflection of guanine microcrystals (M–O) of cells extracted from freshly reef collected corals (left column), from N-depleted corals (middle column) and from the N-depleted symbionts 24 h after the supplementation by guanine powder (right column). Combined images (P–R) illustrate the time evolution of the uptake showing the same cell 10 min (P), 30 min (Q) and 50 min (R) after the addition of guanine. Gradual bleaching of the fluorescence is visible due to laser scanning. Red arrow in images C and O indicate undissolved crystalline guanine outside the cell. Scale bar: 2 μm.

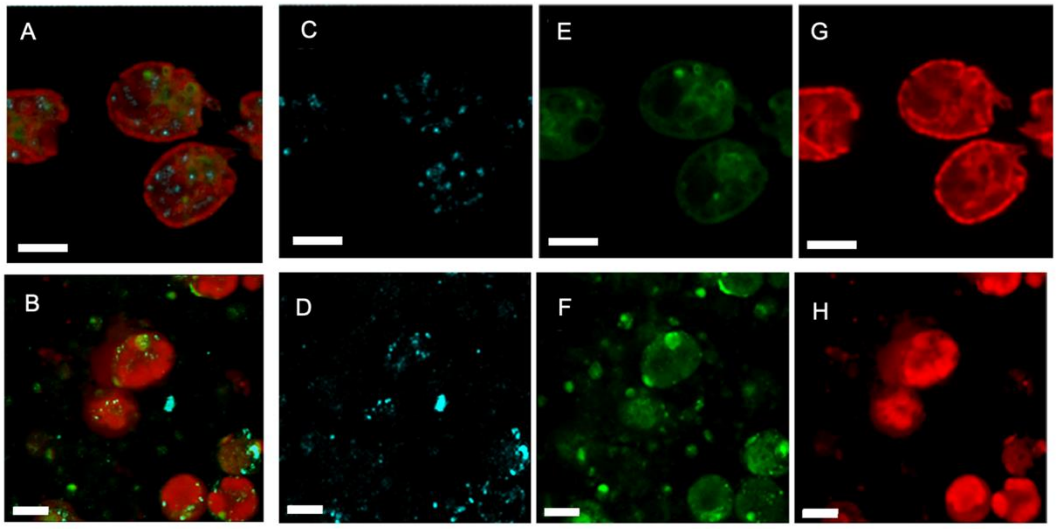


**Fig. S16. (complementing Fig. 7D-F and Fig. S15). Confocal images of *A. carterae* and *Symbiodiniaceae* cells after N feeding.** Confocal images of free-living *A. carterae* cells (A, C, E, G) and *Symbiodiniaceae* cells (B, D, F, H) extracted from reef *Zoanthus* sp. and fed with guanine powder highlighting the crystalline inclusions in a reflection mode of 488 nm laser line (C, D); fluorescence emission at 500 – 560 nm from accumulation bodies and other organelles (E, F); fluorescence emissions of chlorophyll from chloroplasts 670 – 700 nm (G, H); and overlaid combined image (A, B). The presence of crystalline guanine within cells from the same batch was confirmed by Raman microscopy. Scale bar: 5 µm.

**Movie S1 (separate file, complementing Fig. 1) shows a sequence captured in real time by polarization microscopy.** The cover figure shows bright field (A, C) and polarization images (B, D) of an N-starved *A. carterae* cell before (A, B) and 14 minutes after feeding with dissolved guanine (C, D). The video will start upon clicking the cover figure.

**SI Appendix References**


1. S. Rosset, C. D'Angelo, J. Wiedenmann, Ultrastructural Biomarkers in Symbiotic Algae Reflect the Availability of Dissolved Inorganic Nutrients and Particulate Food to the Reef Coral Holobiont. *Frontiers in Marine Science* **2**, 103 (2015).
2. S. Rosset, J. Wiedenmann, A. J. Reed, C. D'Angelo, Phosphate deficiency promotes coral bleaching and is reflected by the ultrastructure of symbiotic dinoflagellates. *Marine Pollution Bulletin* **118**, 180-187 (2017).
3. R. R. L. Guillard (1975) Culture of phytoplankton for feeding marine invertebrates. in *Culture of Marine Invertebrate Animals*, eds W. L. Smith, M. H. Chanley (Plenum Press, New York, USA), pp 26-60.
4. S. H. Yalkowsky, Y. He, P. Jain, *Handbook of Aqueous Solubility Data* (CRC Press, New York, U.S.A., ed. Second, 2010).
5. D. B. Dunn, R. H. Hall, "Purines, Pyrimidines, Nucleosides, and Nucleotides: Physical Constants and Spectral Properties" in Handbook of Biochemistry and Molecular Biology. (CRC Press, 2018), 10.1201/b21846-50 chap. Purines, Pyrimidines, Nucleosides, and Nucleotides: Physical Constants and Spectral Properties.
6. Š. Moudříková *et al.*, Raman and fluorescence microscopy sensing energy-transducing and energy-storing structures in microalgae. *Algal Research* **16**, 224-232 (2016).
7. Š. Moudříková, L. Nedbal, A. Solovchenko, P. Mojzeš, Raman microscopy shows that nitrogen-rich cellular inclusions in microalgae are microcrystalline guanine. *Algal Research* **23**, 216-222 (2017).
8. Š. Moudříková *et al.*, Quantification of polyphosphate in microalgae by Raman microscopy and by a reference enzymatic assay. *Analytical Chemistry* **89**, 12006-12013 (2017).
9. J. W. Eaton, D. Bateman, S. Hauberg, R. Wehbring (2015) GNU Octave version 4.0.0 manual: a high-level interactive language for numerical computations. (CreateSpace Independent Publishing Platform).
10. E. S. Reynolds, The use of lead citrate at high pH as an electron-opaque stain in electron microscopy. *Journal of Cell Biology* **17**, 208-212 (1963).
11. J. M. Delabar, M. Majoube, Infrared and Raman-spectroscopic study of N-15 and D-substituted guanines. *Spectrochimica Acta Part a-Molecular and Biomolecular Spectroscopy* **34**, 129-140 (1978).
12. H. Ishikawa, Hydrolysis of nucleotides by acid. *The Journal of Biochemistry* **22**, 385-395 (1935).
13. H. W. Bischoff, H. C. Bold, *Some soil algae from Enchanted Rock and related algal species*, Phycological studies (University of Texas Publication, Austin, Texas, 1963), vol. IV.
14. V. Zachleder, I. Šetlík, Effect of irradiance on the course of RNA-synthesis in the cell cycle of *Scenedesmus quadricauda*. *Biol Plantarum* **24**, 341-353 (1982).
15. R. Rippka, J. Deruelles, J. B. Waterbury, M. Herdman, R. Y. Stanier, Generic assignments, strain histories and properties of pure cultures of cyanobacteria. *Journal of General Microbiology* **111**, 1-61 (1979).
16. F. Liu, D. E. Hooks, N. Li, N. A. Mara, J. A. Swift, Mechanical properties of anhydrous and hydrated uric acid crystals. *Chem. Mat.* **30**, 3798-3805 (2018).